Preprints (www.preprints.org) | NOT PEER-REVIEWED | Posted: 22 November 2022 doi:10.20944/preprints202211.0398.v1

Disclaimer/Publisher's Note: The statements, opinions, and data contained in all publications are solely those of the individual author(s) and contributor(s) and not of MDPI and/or the editor(s). MDPI and/or the editor(s) disclaim responsibility for any injury to people or property resulting from any ideas, methods, instructions, or products referred to in the content.

Article

Temporal Variability of the Remote Sensing Reflectance and Color Index Trends in the Western Part of The Black Sea

Evgeny Shybanov[1], Anna Papkova[1],Daria Kalinskaya[1]

[1] Marine Hydrophysical Institute of the Russian Academy of Sciences, 2 Kapitanskaya St., 299011 Sevastopol, Russia

* Correspondence:hanna.papkova@gmail.com;

Abstract: Geo-information about the spectral variability of the water-leaving radiance is the key to the validation of satellite and in situ measurements and the development of regional algorithms. In this study, using cluster analysis, five trends were identified that are characteristic of various phenomena in the northwestern part of the Black Sea (summer and winter blooms, turbid waters, river runoff). Typical values of the remote sensing reflectance coefficient are calculated for each case. Additionally, the standard values of the color indices for each cluster are calculated. It is shown that the ratio of the color index *CI*(412/443 nm) is slightly variable and equals 0.8±0.07.This can be a reference point for recovering incorrect (negative) satellite Rrs(λ) values in the shortwave region. In a similar way, the color index was calculated according to the MODIS and VIRS data, it was shown that on days with a turbid atmosphere (high AOT values), the standard deviation of the color index is 30%. For days with a clear atmosphere, the color index is close to the in situ results.

Keywords: water-leaving radiance; remote sensing reflectance; color index; seasonal blooms; AERONET; Black Sea; MODIS Aqua; AOT; VIIRS

1. Introduction

Information about the bio-optical characteristics of sea water is contained in water-leaving radiance that emerged from the water column Lw(λ) [1]. To minimize the variation of ambient light condition, Gordon (1989) introduced the concept of normalized water-leaving radiance L_{WN} as a characteristic of the radiation ascending from the sea surface, which is expressed in terms of Lw(λ) by dividing by the spectral transmission of the descending solar radiation by the atmosphere and the cosine of the solar zenith angle [2]. At the moment, the $L_{WN}(\lambda)$ value is still used as a standard data processing product, but the remote sensing reflectance Rrs(λ) is more often used as the standard product of the atmospheric correction of satellite data, which is calculated as the ratio of the normalized water-leaving radiance to the solar constant. The remote sensing reflectance emerging from the water is determined by the optical properties of sea water, which depend on the quantitative and qualitative composition of the substance contained in it. In this study, it was decided to consider the temporal variability of the in situ remote sensing reflectance in order to estimate the trends of magnitude and their variability for the northwestern part of the Black Sea, which belongs to the type of complex waters (Case 2) [3]. It should be noted that remote sensing methods can measure only the surface layer of water (skin layer).

The value of the remote sensing reflectance coefficient is influenced by many external factors: blooms, river runoff, dissolved organic matter and etc. For example, one of the reasons for the spectral variability of Rrs(λ) could be the bloom of coccolithophorids, a single-celled phytoplankton, the main producer of particulate inorganic carbon (PIC), which significantly affect the carbon balance and, therefore, influence global biogeochemical cycles on short-term and geological time scales [4-5].

© 2022 by the author(s). Distributed under a Creative Commons CC BY license.

Preprints (www.preprints.org) | NOT PEER-REVIEWED | Posted: 22 November 2022 doi:10.20944/preprints202211.0398.v1

Input data to the current research is all AERONET in situ data for two northwestern platforms Gloria and Galata_Platform, which were downloaded at quality level 1.5 (atmospheric correction was carried out) from 2011 to 2022 years. Modern remote sensing algorithms use the normalized brightness $L_{WN}(\lambda)$ or alternatively the remote sensing spectral reflectance $Rrs(\lambda)$ to detect the presence of coccoliths [6-7], estimate the particulate backscatter coefficient $bbp(\lambda)$ and from this the concentration coccoliths and PIC concentration. Recent studies have proposed a direct application of $Rrs(\lambda)$ to determine the concentration of PIC [6]. Several studies have examined the evolution and distribution of coccolithophorid blooms using remote sensing techniques using the Coastal Color Scanner (CZCS) and Wide Field Sea View Sensor (SeaWiFS) imaging [8-9]. For the Black Sea, the region of interest for this study, the SeaWiFS time series for the period 1998–2002 showed a clear coincidence of the so-called June maximum of $L_{WN}(\lambda)$with the flowering of coccolithophores. As already documented, in the western part of the Black Sea there is an almost regular annual bloom of coccolithophores, developing during June and usually gradually disappearing during July [10].

Also for this region, seasonal changes in the species diversity of other phytoplankton types and its numerical characteristics are observed. The spring period was equally represented by diatoms, dinophytes, and golden algae in terms of numbers, however, the main contribution to the phytoplankton biomass in spring was made by dinophytes. Diatoms were represented by typical north-west Black Sea subregion (NWBS) species in spring - Diatomatenuis, Cyclotellacaspia, and for fresh waters - Stephanodiscushantzschii Gran. Among the diatoms, the outbreak of Skeletonemacostatum, a frequent pathogen of water “blooming” in the NWBS during the spring months, was the most severe. In summer, there was a significant increase in the number of blue-greens (up to 91% in abundance and 14% in biomass), which were not found in spring, as well as a slight increase in euglenoids (0.5%). From summer to winter, there was a gradual decrease in biomass, accompanied by a change in the role of individual groups of phytoplankton in its formation. In the autumn months, in the study area, the development of diatoms intensified in the composition of phytoplankton, which accounted for 66% of the total biomass and 58% of the total abundance in autumn. The minimum biomass value was noted in winter, in the formation of which diatoms dominated and accounted for 72%.The contribution of dinophytes (26%) and occasional blue-green algae (1%) decreased [11]. Seasonal dynamics of the abundance of various phytoplankton species based on the results of statistical analysis is presented in Table 1.

Table 1. Seasonal dynamics of abundance (thousand cells l-1) of phytoplankton in the NWBS in 2005-2013

Season	Diatoms	Dinophytes	Blue-green	Golden
Spring	220.50	392.4	0	390.3
Summer	83.54	127.8	2628.93	3.04
Autumn	46.10	15.85	14.7	1.15
Winter	287.50	24.90	3.4	0.5

Also, the seasonal variability of $Rrs(\lambda)$ values in a given area can be significantly affected by river runoff. Given the regional division of the Black Sea based on bathymetry and river flow, the AERONET-OC areas of interest for study (i.e. Galata and Gloria/Section-7) are located on the northwestern and southwestern inland shelves. Both these regions are characterized by high variability of optically complex waters [12] as a result of the joint influence of local dynamics and the runoff of the Danube, Dnieper, Dniester, and Buga rivers. Judging by the time series from 1991 to 2008, the Danube runoff usually peaks between late April and early May [13], when coccolithophorid

Preprints (www.preprints.org) | NOT PEER-REVIEWED | Posted: 22 November 2022 doi:10.20944/preprints202211.0398.v1

blooms can already occur and significantly affects the change in values the brightness of the sea (Figure 1).

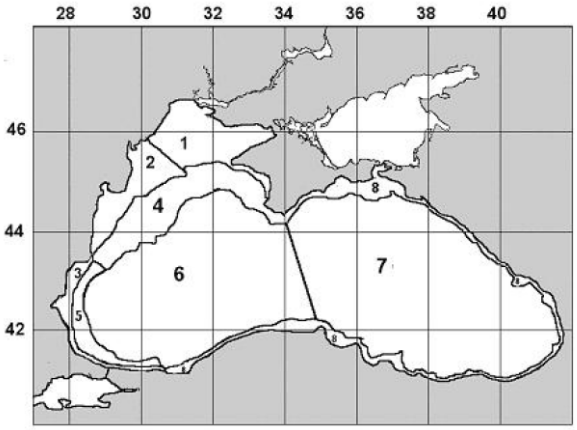

Figure. 1. Sub-regions in the Black Sea: 1 - northern inner shelf (depths less than 50 m); 2-north-western inner shelf (depths less than 50 m); 3-southwestern inner shelf (depths less than 50 m); 4-north-western outer shelf (depths 50-200 m); 5-south-western outer shelf (depths 50-200 m); 6-western open part (depths over 200 m); 7-eastern open part (depths over 200 m); 8-eastern and southern shelf (depths less than 200 m).

For the Black Sea, 8 subregions have been identified [3]. Six of them (1-5 and 8) belong to the shelf area (depth less than 200 m), sub-regions 6 and 7 are open deep sea areas (Fig. 1). In the shelf area, sub-regions are distinguished according to their position, bathymetry, and the influence of river runoff. Sub-regions 1-3 are the inner shelf with depths less than 50 m; sub-region 1 is influenced by the river flow of the Dnieper, Bug and Dniester, while sub-region 2 is influenced by the Danube.

Thus, for this area, it is interesting to highlight trends in variability under the influence of external factors.

2. Materials and Methods

One of the most effective sources of studying the characteristics of atmospheric aerosol, as well as in situ measurements of ocean color, is the global network of observational ground-based automated stations (platforms) AERONET (Aerosol ROboties NETwork).For the entire period of operation within the framework of the AERONET network, the Black Sea region was represented by 4 regularly measuring stations: Sevastopol (44.616N, 33.517E), Gloria (44.600N, 29.360E), Galata_Platform (43.045N, 28.193E) and Eforie (44.075N, 28.632 e). However, not all stations have now continued to operate within this network: the Sevastopol station ceased to function in 2015, and the Gloria station has been replaced by a backup station Section-7_Platform since 2019 (Figure 2.).

Preprints (www.preprints.org) | NOT PEER-REVIEWED | Posted: 22 November 2022 doi:10.20944/preprints202211.0398.v1

Figure 2. Location of AERONET stations for the Black Sea region.

Gloria AERONET-OC (29.36°E, 44.60°N), established in 2010 on a Petrom-owned and operated gas platform of the same name, is located approximately 12 nautical miles off the Romanian coast south of the Danube Estuary . In August 2019, this site was decommissioned and replaced by Site-7 (29.45°E, 44.45°N), a gas platform also owned and operated by Petrom and located a few nautical miles south of Gloria. The water depth in both places is about 40 m. The Galata_Platform AERONET-OC site (28.19°E, 43.05°N), established in 2014 on the gas platform of the same name, owned and operated by Melrose, is located approximately 13 nautical miles off the coast of Bulgaria in front of the city of Varna. The water depth in this area is 35 m.

The AERONET network, developed for atmospheric research at various scales, has been expanded to support marine applications. This new network component, called AERONET - Ocean Color (AERONET-OC), provides an additional capability to measure the water-leaving radiance. AERONET-OC plays an important role in ocean color satellite activities through standardized measurements that are a) performed at different locations using a single measurement system and protocol, b) calibrated using an identical reference source and method, and c) processed using the same code. At the moment, only two Black Sea stations provide information on the ocean color according to the measurements of Section-7_Platform (in past: Gloria) and Galata_Platform stations. For the western part of the Black Sea, data on the water-leaving radiance (Lw) are regularly provided, as well as the normalized water-leaving radiance (L_{WN}) calculated by the method proposed by Zibordi et al. [14] to remove the dependence on survey geometry and bidirectional effects in Lw. It is worth noting, since in the future satellite and in situ measurements of the water-leaving radiance will be validated and all values of $L_{WN}(\lambda)$ will subsequently be converted to Rrs(λ) by dividing by the solar constant Fo(λ):

$$Rrs(\lambda) = L_{WN}(\lambda)/Fo(\lambda). \quad (1)$$

The source of satellite measurements of Rrs(λ) was the results of MODIS-Aqua spectroradiometer measurements. MODIS-Aqua has 36 spectral channels, but only 9 of them were originally related to the ocean color (including the 673-683 nm channel, designed to detect chlorophyll fluorescence excited by solar radiation), the rest are designed to study the atmosphere and land and determine temperature surfaces and clouds. MODIS has radiometric sensitivity in 36 spectral channels in the spectral range from 0.4 to 14.4 μm. Based on the measurement data in all MODIS spectral channels, a standard set of 44 values is calculated, including calibrated radiances at the upper boundary of the atmosphere, tied in time and coordinates, and various geophysical parameters. For monitoring the state of the ocean, the most interesting are the aerosol optical depth, the optical thickness and height of clouds, the concentration of chlorophyll, the concentration of suspended particles and the dispersion index of marine suspension, the absorption index of sea water, as well as day and night temperature of the ocean surface.

AERONET results were additionally checked for compliance with the model remote sensing reflectance, which are linearly dependent on the ratio of light backscattering by sea water to absorption. The model value of Rrs(λ)$\cdot\pi$ should be written as [15]:

$$\rho(\lambda) = s \cdot b_b(\lambda)/a(\lambda)$$

where s is the coefficient of proportionality depending on the phase function, more precisely on the geometry and observation conditions. We used the value s = 0.15. Backscattering, in turn, can be described by formula as [16]:

Preprints (www.preprints.org) | NOT PEER-REVIEWED | Posted: 22 November 2022 doi:10.20944/preprints202211.0398.v1

$$b_b(\lambda) = b_{bw}(\lambda) + b_{bp}(\lambda_0)\frac{\lambda_0}{\lambda}$$

Absorption was written as a sum of three terms with two unknowns [17]:

$$a(\lambda) = a_w(\lambda) + C_{chl}a^*_{ph}(\lambda) + C_{ddm}e^{-0.015(\lambda-\lambda_0)}$$

where is the C_{chl} concentration of chlorophyll, C_{ddm} is the concentration of organic matter, detritus + yellow matter, a_w is the absorption rate of pure water, a_{ph} is the specific absorption index of phytoplankton according to the model described in [18] at a given concentration of chlorophyll C_{chl}=0.75 mg/m3, corresponding to the data of the work [19].

Next, a search was made for the minimum residual of the model and in situ Rrs(λ) values with its allowable limit values, the value of the residual should not exceed . 87% of all values provided by AERONET were consistent with this model. The remaining emissions may be associated with the non-accounting for polarization during measurements, the error in accounting for the reflected component (heterogeneity of the sky, waves, polarization).

Remote sensing reflectance (Rrs(λ)) (sr-1), for MODIS data is determined for spectral channels 412, 443, 469, 488, 531, 547, 555, 645, 667, 678 nm. The concentration of chlorophyll a, (mg m-3) according to MODIS data is calculated using Rrs(λ) values for 2-4 wavelengths from the range of 440-670 nm [20-22]. In this study, we use satellite data to calculate the color index(CI) at 412 and 443 nm.

As a follow-up VIIRS instrument, VIIRS-NOAA-20 is essentially built in the same manner as VIIRS-SNPP. Therefore, the sensor characteristics of the two instruments are very similar. Both SNPP and NOAA-20 operate in the 824-km Sun-synchronous polar orbit, which crosses the equator at about 13:30 local time. There is about a 50-min delay between the paths of NOAA-20 and SNPP, which makes the NOAA-20's path run through the middle of 2 adjacent SNPP paths, and vice versa. The overlap of the spatial coverages of the two sensors automatically fills each other's gaps caused by high sensor-zenith angles and high Sun glint contamination, and it significantly reduces the missing pixels in the merged images. In addition, the ocean color products from SNPP and NOAA-20 have the same spatial and temporal resolution and are processed with the same software package, i.e., the Multi-Sensor Level-1 to Level-2 (MSL12) ocean color data processing system [23-26]. Therefore, the statistics of their ocean color products are very similar, and in fact, the data can be directly merged without adjustment to match with each other's statistical properties. However, much data is still missing in the merged VIIRS SNPP/NOAA-20 products [26]. In current research, we also calculated the color index at 410 and 443 nm.

3. Results

In the northwestern part of the Black Sea, there are 2 AERONET stations, each of which provides the total number of measurements (for Galata-8841 and Gloria - 7171), it was proposed to analyze the average daily values of the Rrs(λ) using the criterion of variability of daily measurements in the short-wavelength region of the spectrum. The ratio of the standard deviation of all measurements per day to the average value of the Rrs(λ) for the same day at 412 nm should not exceed 10%. Going forward, this step will help eliminate outliers and data with strong variability, which may indicate poor experimental conditions. Thus, about 42% of all dates on which measurements were taken were screened out, especially large daily variability was observed in November-February, possibly due to adverse weather conditions. To analyze the seasonal variability of the Rrs(λ), 553 dates from 2013 to 2022 were selected for the Galata_Platform station, and 408 dates from 2011 to 2019 for the Gloria station.

Preprints (www.preprints.org) | NOT PEER-REVIEWED | Posted: 22 November 2022 doi:10.20944/preprints202211.0398.v1

Consequently, the analyzed sample comprised 961 spectra of the brightness coefficient Rrs(λ) on 10 channels (412 nm, 443 nm, 490 nm, 510 nm, 532 nm, 551 nm, 555 nm, 667 nm, 870 nm, 1020 nm).

We propose to identify various typical trends in the variability of the remote sensing reflectance by performing a cluster analysis of the entire dataset.Cluster analysis was carried out in the Python software package using the K-Means function. In this type of algorithm, the data is divided or divided into "K separate clusters". It is necessary to choose the number of clusters (K) according to the data (in this case we use 6 clusters). Cluster centers will be optimized based on the average of the points assigned to the given cluster. If the centroids of the clusters do not move much or move only a small distance, we can say with certainty that the K-means cluster converges. With the help of cluster analysis, seasonal values of the Rrs(λ) with trends were considered in the presence of blooms or the influence of river runoff. The general distribution of the number of studied dates by season for each AERONET station is presented inFigure 3.The dominant amount of data corresponds to the summer period, the least in winter (presumably due to adverse weather conditions due to high wind speed, heavy cloudiness).

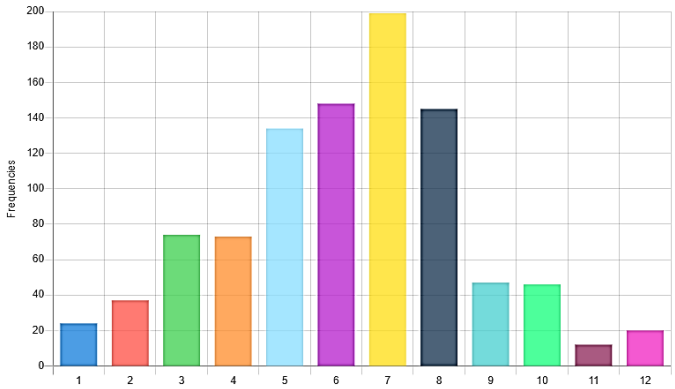

Figure 3. Histogram of the frequencies of the month's distribution of the AERONET data array for the northwestern part of the Black Sea

Bloom events were investigated using the spectral features resulting from the scattering of coccolithophorid using an algorithm originally proposed for CZCS and SeaWiFS images [6]. This algorithm sets a flag, hereinafter referred to as the coccolith flag, based on the conditions applied to the spectral values of $L_{WN}(\lambda)$ and their ratios:

$$g_{coccoliths} = \begin{cases} L_{wn}(443) > 1.1 \\ L_{wn}(555) \geq 0.9 \\ 0.75 < \frac{L_{wn}(443)}{L_{wn}(555)} < 1.85 \\ 1.0 < \frac{L_{wn}(510)}{L_{wn}(555)} < 1.65 \\ 0.6 < \frac{L_{wn}(443)}{L_{wn}(510)} < 1.15 \end{cases} \quad (2)$$

Since Galata_Platform station does not provide data at 510 nm and 555 nm (but there are nearest channels at 490 nm, 532 nm and 551 nm), and for Gloria 510 nm with gaps at 555 nm, it was decided to interpolate data from a set of 10 points (412nm, 443nm, 490nm, 510nm, 532nm, 551nm, 555nm, 667nm, 870nm, 1020nm) in Python as a 2nd degree polynomial function. Therefore, after cluster analysis, the following result (centroids of Rrs(λ))was obtained Figure 4.

Preprints (www.preprints.org) | NOT PEER-REVIEWED | Posted: 22 November 2022 doi:10.20944/preprints202211.0398.v1

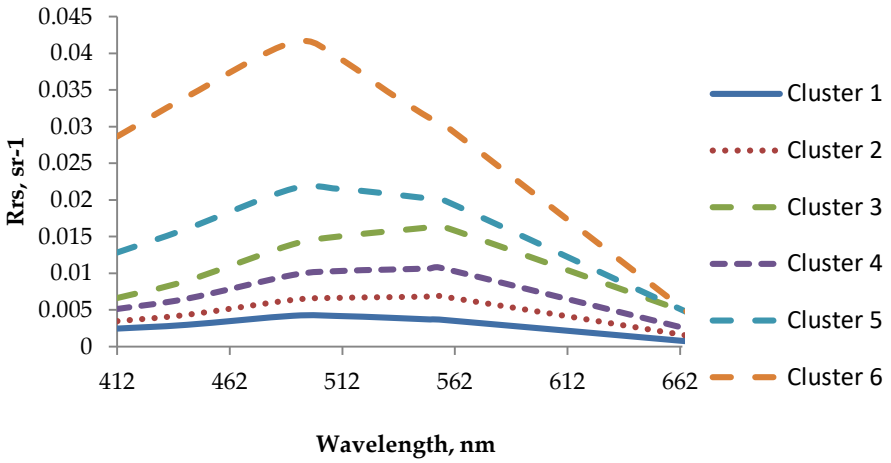

Figure 4. Spectral behavior of centroids Rrs(λ) for 6 clusters (Black Sea area).

For each cluster, an analysis of Rrs(λ) variability, finding the maximum of the spectrum, as well as a constant frequency histogram by months was carrying out(Figure 5).

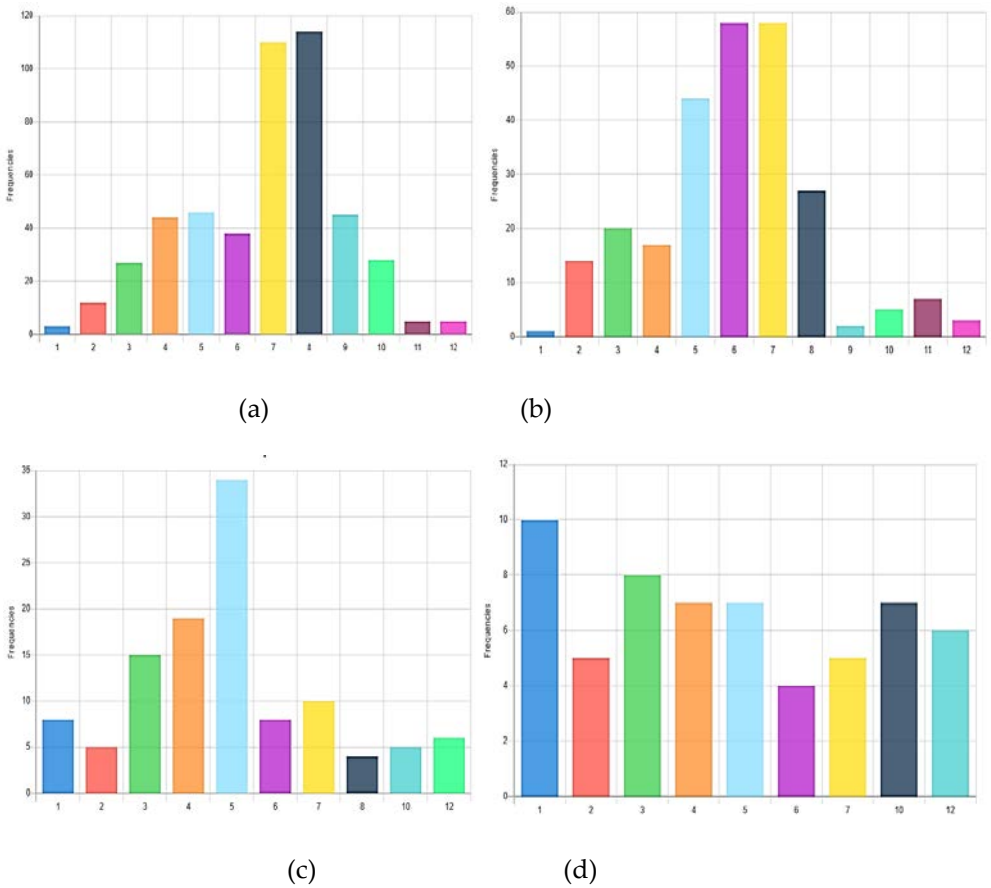

(a) (b)

(c) (d)

Figure 5. Frequency histogram by months for (a) Cluster 1; (b) Cluster 2;

(c) Cluster 3; (d) Cluster 4.

Cluster 1. This cluster contains the largest number of values, namely 477, which is 49% of the total data. The values of the remote sensing reflectance in this case are the smallest, while the maximum of the spectrum is in the region of 490 nm. It can be seen from the histogram of the distribution of frequencies by months that fell into this cluster that this

Preprints (www.preprints.org) | NOT PEER-REVIEWED | Posted: 22 November 2022 doi:10.20944/preprints202211.0398.v1

mode is present throughout the year, with the highest frequency in July and August (Figure 5 (a)).We assume that this cluster contains "typical" (close to expeditionary values in the central part of the Black Sea) brightness coefficients for the northwestern part of the Black Sea in the absence of blooms in sea water, while the water is not very turbid. The minimum values of the remote sensing reflectance at 412 nm were calculated as the average value of Rrs(λ) minus the standard deviation and equaled 0.0016. This information is necessary for the correct reconstruction of satellite Rrs(λ) in the presence of an absorbing aerosol.

Cluster 2. This cluster contains 256 values, which is 27% of the total data. The values of the remote sensing reflectance in this case are also quite low, but the maximum of the spectrum is in the region of 555 nm, which is an indicator of turbid water. From the histogram of the distribution of frequencies by months that fell into this cluster, it can be seen that this mode is present throughout the year, with the highest frequency in June and July (Figure 5 (b)).

Cluster 3. The third cluster contains 117 values (12% of the total sample), the Rrs(λ) values increase by more than 2 times compared to the first cluster, the shift of the spectrum maximum by 555 nm (turbid water indicator). There are clear trends from the end of March to the beginning of June (Figure 5 (c)), we assume that this cluster may show the influence of river runoff, since the Gloria AERONET-OC site is located approximately 13 nautical miles from the coast of Romania south of the mouth Danube.

Cluster 4. This cluster contains 59 values (6%). It is characterized by even higher values of Rrs(λ) and a maximum of the brightness spectrum at 555 nm. The frequency histogram by months showed clear peaks in winter and off-season (Figure 5 (d)). Most likely, this cluster corresponds to the winter bloom of phytoplankton (diatoms and dinophytes).

Clusters 5 and 6. Cluster 5 contains 44 points (5%), cluster 6 has only 6 points (0.6%). These groups correspond to the flowering period of coccolithophorids. All reported cases were reported from late May to July. When calculating the color index system (formula 2), the fact of flowering was additionally confirmed. In these clusters, the highest values of the remote sensing reflectance for all wavelengths were noted with a spectral maximum at 490 nm, which is in good agreement with [11]. Cluster 6 represents the flowering of coccolithophorids in the absence of dissolved organic matter. The minimum values of the remote sensing reflectance at 412 nm were calculated as the average value of Rrs(λ) minus the standard deviation and equaled 0.009. This information is necessary for the correct reconstruction of satellite Rrs(λ) in the case of the presence of absorbing aerosol in the presence of strong blooms in summer in the northwestern Black Sea.

Consequently, the centroids of the first cluster can be considered the closest to the "typical" values of the remote sensing reflectance in the northwest of the Black Sea. Turbid waters include the results of the 2nd cluster, the 3rd cluster, most likely, demonstrates the trends in Rrs(λ) change under the influence of river runoff. We assume that cluster 4 refers to the autumn-winter blooms of diatoms and dinophytes, and clusters 5 and 6 to the summer blooms of coccolithophores.

Based on the cluster data, an additional analysis was made of various combinations of color indices used in the Ocean Color algorithms to find the concentration of chlorophyll-A (Table 3). Detailed information on the procedure for finding Chl-a is described at[27-28].

Preprints (www.preprints.org) | NOT PEER-REVIEWED | Posted: 22 November 2022 doi:10.20944/preprints202211.0398.v1

Table 3. Average values of color indexes with standard deviations for different clusters by AERONET stations (Galata, Gloria)

Cluster	CI(412/443)	CI(443/555)	CI(443/488)	CI(443/547)
1	0.83±0.07	0.8±0.3	0.70±0.08	0.77±0.26
2	0.73±0.07	0.54±0.2	0.64±0.07	0.57±0.16
3	0.79±0.08	0.60±0.2	0.66±0.07	0.62±0.17
4	0.80±0.07	0.60±0.2	0.68±0.06	0.64±0.20
5	0.79±0.06	0.8±0.2	0.75±0.06	0.78±0.17

As can be seen from Table 3, the ratio *CI*(412/443) changes slightly and is approximately equal to 0.79. In the future, this will be used to restore the values at 412 nm during the procedure for additional correction of the satellite values of Rrs(λ) in the presence of obvious errors (for example, negative values in the shortwave region).

In the first case, a cluster analysis was presented without taking into account the shift in the maximum of the remote sensing reflectance, and also without additional verification of the data. If we calculate the maxima for each spectrum and add them as another criterion for data clustering (K-Means procedure), 5 explicit groups are distinguished. Cluster 1 contains 219 values, maximum at 540 nm. The values of Rrs(λ) are not high, the mode is determined throughout the year. This group corresponds to turbid waters. Cluster 2 contains 130 values, the maximum is at 490 nm, the values of the central Rrs(λ) are high, the peak is from May to August, presumably this group is associated with the flowering of coccolithophorids. Cluster 3 (164 values) represents very turbid waters, since the maximum wavelength is at 565 nm. Fashion is present in the spring-summer period. The Rrs(λ) are low in the short-wavelength region of the spectrum and very high in the green part of the visible region, this may also be associated with blooms, or with a high concentration of mineral suspension (sand, clay). Cluster 4 represents the values of the spectral coefficient of brightness of the sea, close to the values in the central part of the Black Sea. Presumably, cluster 5 corresponds to winter flowering in the off-season as well.When recalculating the color indices for the new cluster separation, we found that the ratio CI(412/443) changes slightly and is approximately equal to 0.81±0.07, which practically corresponds to the results of the previous cluster analysis, without taking into account the shift of the model maximum Rrs(λ). In general, CI(412/443) for the western part of the Black Sea varies from 0.79 to 0.81. Regardless of the degree of change in turbidity, the ratio on the two channels remains approximately constant; this can be used to build atmospheric correction algorithms using the short-wavelength visible region.

If we calculate the color index without clustering, the mode is still visible (Figure 6).

Preprints (www.preprints.org) | NOT PEER-REVIEWED | Posted: 22 November 2022 doi:10.20944/preprints202211.0398.v1

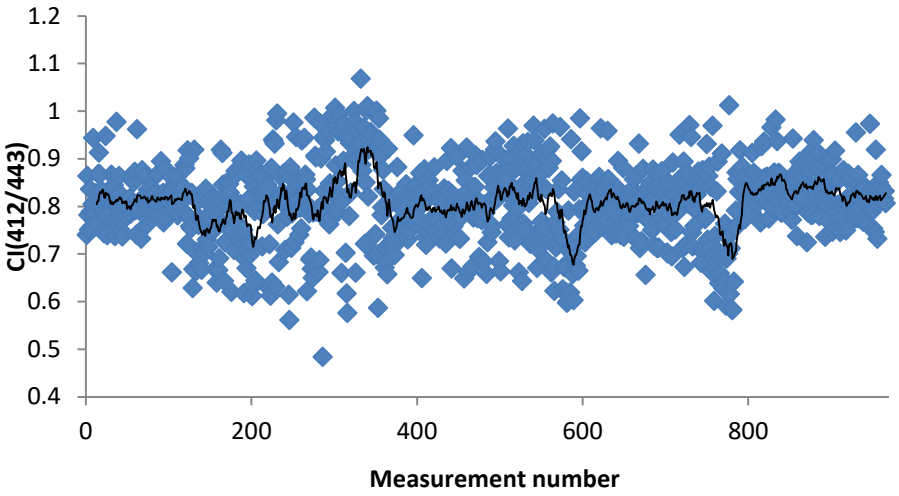

Figure 6. Variability of calculated CI(412/443) values based on in situ data from Gloria and Galata Platform from 2011 to 2022.

The average value of CI(412/443) = 0,80±0,08, a small standard deviation indicates that the sample is slightly variable. It is worth noting that the median of the sample is also at 0.80, which indicates an ideal symmetrical distribution. For other color indices using the green region of the spectrum (for example, 443/547 or 488/547), little variability was observed, RMS values >20%.We calculated the color indices for the MODIS Aqua and VIIRS SNPP data for Gloria and Galata Platform coordinates with further calculation of the mean value and standard deviation. We also divided the satellite data into two groups: days with a clean atmosphere (low values of the aerosol optical thickness (AOT) and days with an inhomogeneous (turbid) atmosphere (high AOT).Figure 7 shows the course of CI(412/443) points depending on the turbidity of the atmosphere for Modis Aqua data.

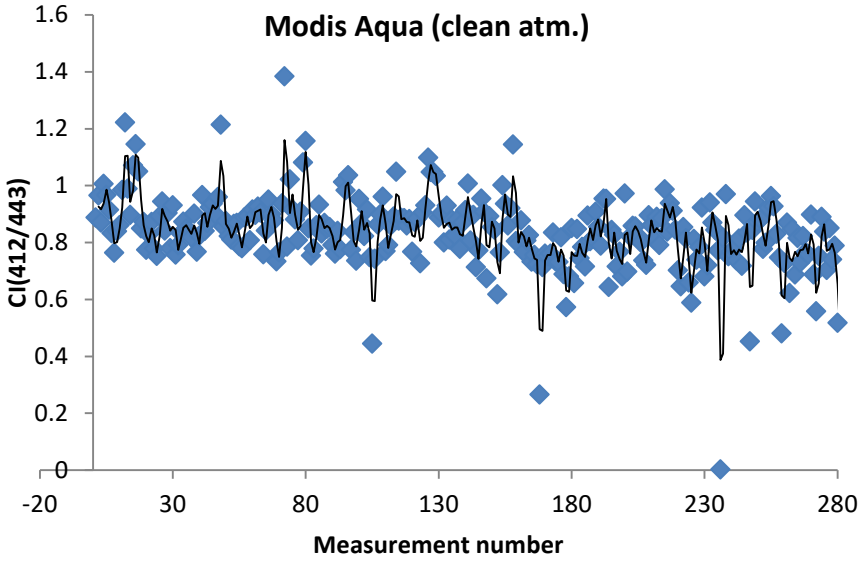

(a)

Preprints (www.preprints.org) | NOT PEER-REVIEWED | Posted: 22 November 2022 doi:10.20944/preprints202211.0398.v1

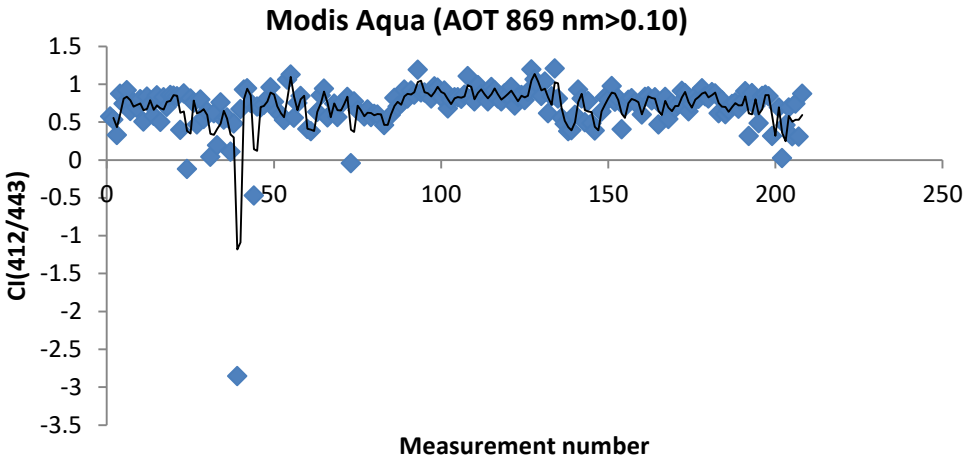

(b)

Figure 7. Variability of calculated CI(412/443) values based on in satellite MODIS Aqua data to Gloria and Galata Platform coordinates (a) all cases, (b) with high AOT.

In cases of clean atmosphere, the average value of CI(412/443 nm) for Modis Aqua data is 0,836±0,13 which is close to in situ values. For turbid days it is equal 0,70±0,34. An increase in the standard deviation indicates atmospheric correction errors. Similarly, for VIIRS SNPP data we get 0.82±0.13 for days with small AOT and 0.50±0.44 for inhomogeneous (turbid) atmosphere. Thus, the value of the color index CI(412/443) = 0,80±0,08,can be used as a reference for the development of additional algorithms for atmospheric projection and where it is necessary to take into account the short-wavelength region of the spectrum.

4. Discussion

Information about the temporal variability of the remote sensing reflectance of the sea is necessary for Ocean Color problems and for development of regional algorithms. It is known that atmospheric correction errors are affected by many factors, (for example spatial inhomogeneity of the atmosphere, presence of absorbent aerosol) and strongly affect the standard Ocean Color products. It was previously shown that often for the Black Sea, the results of Rrs(λ) at 412 and 443 nm are not informative, since they have large errors. For example, very often during the presence of dust transport over the Black Sea region, the values at 412 nm were negative [29-30].The availability of information about the features of light reflection by the sea in the blue region would make it possible to significantly improve the accuracy of atmospheric correction in other spectral channels, since in the case of the presence of an absorbing aerosol, the satellite values of Rrs(λ) at 412 nm can often take negative values. Previously, it was proposed to consider the reflectance constant in the short-wavelength region of the spectrum [31]. It was shown in [31] that absorption by impurities and scattering by suspended particles change monotonically, except for the absorption band of chlorophyll (approximately 420 – 460 nm). The observed linear relationship between these values shows that they do not depend on the third parameter, specifically on the concentration of chlorophyll-a. Therefore, outside its absorption band, a simplified relationship can be established between them. We propose to determine the value of remote sensing reflectance in the blue region (for satellite measurements - at a wavelength of 412 nm) according to a certain "standard spectrum" of it, which is calculated based on the "typical" value of Rrs(λ) at 412 nm, obtained in the course of cluster analysis in situ measurements.

Preprints (www.preprints.org) | NOT PEER-REVIEWED | Posted: 22 November 2022 doi:10.20944/preprints202211.0398.v1

The minimum values of the brightness coefficient Rrs spectra of the water surface at the wavelengths of the maxima of absorption of solar radiation by chlorophyll-a (443 nm) and additional pigments (488 nm) are observed during the flowering of algae common in the seas and oceans[32-34]. The brightness coefficients Rrs(443) and Rrs(412) depend on the abundance of colored dissolved organic matter of natural origin (CDOM), suspended particles of different nature, atmospheric correction errors and other conditions that control the level and spectral course of Rrs estimates [35].The minimum values of the remote sensing reflectance at 412 nm were calculated as the average value of Rrs(λ) for the first cluster (BS clear water) minus the standard deviation and was equal to 0.0016.Similarly, one can recover values in the shortwave region using color index ratios. In the course of cluster analysis, it was shown that, regardless of external factors, the ratio *CI*(412/443) is practically unchanged and amounts to 0.79 with a standard deviation of 0.07.It is also possible to use the similar procedure of cluster analysis and calculation of "typical" minima or color indices for other water areas where regular calculations of in situ values of the remote sensing reflectance are provided (for example, from other AERONET coastal platforms).At the moment, our research team has already developed the initial version of the algorithm, which will allow us to restore bad quality data, for example, on days of dust transfers, based on the constancy of the color index *CI*(412/443), more information is contained in the [36].

Author Contributions: Conceptualization, E.B.S. and A.S.P.; methodology E.B.S. and A.S.P.; formal analysis, A.S.P. and E.B.S.; investigation, A.S.P. and E.B.S.; data curation, A.S.P. and E.B.S.; writing—original draft preparation, A.S.P. and D.V.K.; writing—review and editing, E.B.S., A.S.P.and D.V.K.; visualization A.S.P and D.V.K.. All authors have read and agreed to the published version of the manuscript.

Funding: The work was carried out within the framework of the state task theme No. 0555-2021-0003 “Development of methods operational oceanology based on interdisciplinary studies of the processes of formation and evolution of the marine environment and mathematical modeling with the use of data from remote and contact measurements” (code “Operational Oceanology”).

Data Availability Statement: The data presented in this study are available on request from the corresponding author.

Acknowledgments: The authors thank Giuseppe Zibordi for processing of measurements obtained at the Galata_Platform and Gloria AERONET stations, and for the possibility of using high-quality in situ ocean color measurements. We also want to thank the Ocean Color processing group.

Conflicts of Interest: The authors declare no conflict of interest.

References

1.Werdell, P. J.; Bailey, S. W. An improved bio-optical data set for ocean color algorithm development and satellite data product validation. *Remote Sensing of Environment*. 2005,V.98, pp. 122-140, https://doi.org/10.1016/j.rse.2005.07.001

2. Gordon, H.R. Can the Lambert-Beer low be applied to the diffuse attenuation coefficient of ocean water. *Limnology and Oceanography*. 1989, V. 34, No. 8, pp. 1389-1409.

3. Kopelevich, O.V.;Sheberstov, S.V.;Yunev, O.;Basturk, O.;Finenko, Z.Z.;Nikonov, S.;Vedernikov, V.I. Surface chlorophyll in the Black Sea over 1978-86 derived from satellite and in situ data.*J. Mar. Systems.* 2002, V. 36, No. 3-4, pp. 145-160.

4. Balch, W.M.; Drapeau, D.T.; Bowler, B.C.; Lyczskowski, E.; Booth, E.S.; Alley, D. The contribution of coccolithophores to the optical and inorganic carbon budgets during the Southern Ocean Gas Exchange Experiment: new evidence in support of the Great Calcite Belt hypothesis. *J. Geophys. Res. Ocean*. 2011,V. 116, pp. 1-14.

5. Müller M.N. *O*n the genesis and function of coccolithophore calcification. *Front. Mar. Sci.* 2019**,** V.6, p. 49.

6. Iglesias-Rodríguez, M.D.; Brown, C.W.; Doney,S.C.; Kleypas, J.; Kolber, D.; Kolber, Z.; Hayes, P.K.; FalkowskiP.G. Representing key phytoplankton functional groups in ocean carbon cycle models: coccolithophorids. *Glob. Biogeochem. Cycl*. 2002**,** *V.*16, https://doi.org/10.1029/2001gb00145447-1-47-20

Preprints (www.preprints.org) | NOT PEER-REVIEWED | Posted: 22 November 2022 doi:10.20944/preprints202211.0398.v1

7. Moore, T.S.; Dowell, M.D.; Franz B.A. Detection of coccolithophore blooms in ocean color satellite imagery: a generalized approach for use with multiple sensors. *Remote Sens. Environ.* 2012, V.117, pp. 249-263, doi:10.1016/j.rse.2011.10.001

8. Brown, C.W.; Yoder, J.A. Coccolithophorid blooms in the global ocean. *J. Geophys. Res.***1994**, V.99, pp. 7467-7482, https://doi.org/10.1029/93JC02156

9. Cokacar, T.;Kubilay, N.;Oguz,T. Structure of Emilianiahuxleyi blooms in the Black Sea surface waters as detected by Sea WIFS imagery. *Geophys. Res. Lett.***2001**, V.28, pp. 4607-4610, https://doi.org/10.1029/2001GL013770

10. Kopelevich, O.V.;Burenkov, V.I.;Sheberstov, S.V.;Vazyulya, S.V.;Kravchishina, M.D.;Pautova, L.;Silkin, V.A.;Artemiev, V.A.;Grigoriev V. Satellite monitoring of coccolithophore blooms in the Black Sea from ocean color data. *Remote Sensing of Environment.* 2014, V. 146, pp. 113–123.

11. Lobkov, V.A.Odessa region of the Black Sea: hydrobiology of the pelagic and benthal. *IMB Monographies.* 2017,p.320.

12. Zibordi, G.; Mélin, F.;Berthon, J.F.; TaloneM. In situ autonomous optical radiometry measurements for satellite ocean color validation in the Western Black Sea. *Ocean Sci.* 2015,V.11, pp. 275-286, 10.5194/os-11-275-2015

13. Stagl, J.C.; Hattermann, F.F. Impacts of Climate Change on the Hydrological Regime of the Danube River and Its Tributaries Using an Ensemble of Climate Scenarios. *Water 2015*, 7, 6139-6172. https://doi.org/10.3390/w7116139

14. Zibordi, G.; Holben, B.; Slutsker, I.; Giles, G.; D'Alimonte, D.; Melin, F.; Berthon, J. F.; Vandemark, D.; Feng, H.; Schuster, G.; Fabbri, B. E.; Kaitala, S.; and Seppala, J. AERONET-OC: A Network for the Validation of Ocean Color Primary Products. *J. Atmos. and Oceanic Technology*2009, V. 26, 1634-1651, https://doi.org/10.1175/2009JTECHO654.1

15. Kopelevich, O.V. Low-parameter model of the optical properties of seawater. *OptikaOkeana; Nauka: Moscow*, Russia, 1983; Volume 1, pp. 208–234.

16. Morel, A. Diffusion de la lumière par les eaux de mer: Résulatsexpérimentaux et approchethéorique, *AGARD, Lecture series,* 1973, Vol.61, pp.31.1 – 31.76.

17. Smith R.C. Optical properties of clearest natural waters (200-800 nm), *Appl. Optics*, 1981, Vol. 20, pp. 177–184.

18. Bricaud, A., Babin,M., Morel, A., Claustre. Variability in the chlorophyll–specific absorption coefficients of natural phy-to-plankton: Analysis and parameterization, *J. Geophys. Res*, 1995, Vol. 100, pp. 13321–13332.

19. Churilova, T.YA. Pogloshcheniyesvetafitoplanktonom, detritom i rastvorennymorganicheskimveshchestvom v pribrezhnomrayoneChernogomorya (iyul' – avgust 2002 g), *Morskoygidrofizicheskiyzhurnal*, 2004, Vol. 4, pp. 39–50.

20. Kopelevich, O. V., Saling, I. V. Interannual changes in bio-optical characteristics of the seas of Russia according to satellite data in 2016-2018. *Proceedings of the X Anniversary All-Russian Conference "Modern problems of optics of natural waters".* 2019, pp. 106-113.

21. Kopelevich, O. V., Sheberstov, S. V., Burenkov, V. I., Vazyulya, S. V., Sahling, I. V.. Bio-optical characteristics of the Russian Seas from satellite ocean color data of 1998-2012. *Current problems in optics of natural waters*, 2013. pp. 168-171.

22. Salyuk, P., Bukin, O., Alexanin, A., Pavlov, A., Mayor, A., Shmirko, K., Krikun, V.. Optical properties of Peter the Great Bay waters compared with satellite ocean colour data. *International Journal of Remote Sensing*, 2010, 31(17-18), pp. 4651-4664.

23. O'Neill, N.T.; Dubovik, O.; Eck, T.F. A modified Angstrom coefficient for the characterization of sub-micron aerosols. *Appl. Opt*.2001, 40(15), 2368–2375. https://doi.org/10.1364/AO.40.002368

24. Joel,P.; Scottand, P.; Werdell, J., Comparing level-2 and level-3 satellite ocean color retrieval validation methodologies.*Opt Express*. 2019, 27, 30140-30157

25. Xiaoming, Liu; Menghua, Wang. Filling the Gaps of Missing Data in the Merged VIIRS SNPP/NOAA-20 Ocean Color Product Using the DINEOF Method.*Remote Sens*. 2019, 11, 178; doi:10.3390/rs11020178

26. Seegers, Bridget N., Richard P. Stumpf, Blake A. Schaeffer, Keith A. Loftin, and P. Jeremy Werdell (2018), Performance metrics for the assessment of satellite data products: an ocean color case study. *Optics Express*. Vol. 26, No. 6, 7404-7422, DOI: 10.1364/OE.26.007404

Preprints (www.preprints.org) | NOT PEER-REVIEWED | Posted: 22 November 2022 doi:10.20944/preprints202211.0398.v1

27. Hu, C.; Lee, Z.; Franz, B. Chlorophyll a algorithms for oligotrophic oceans: A novel approach based on three-band reflectance difference . *Journal of Geophysical Research*2012, V.117(C1). https://doi.org/10.1029/2011jc007395

28. O'Reilly, J.E.; Maritorena, S.;Mitchell, B. G.; Siegel, D. A.; Carder, K. L.; Garver, S. A.; Kahru, M.; McClain, C. R. Ocean color chlorophyll algorithms for SeaWiFS.*Journal of Geophysical Research* 1994, V. 103, pp. 24937-24953, https://doi.org/10.1029/98JC02160

29. Kalinskaya, D.V.; Papkova, A.S. Why Is It Important to Consider Dust Aerosol in the Sevastopol and Black Sea Region during Remote Sensing Tasks? A Case Study. *Remote Sens.* 2022, *14*, 1890. https://doi.org/10.3390/rs14081890

30. Suetin, V.S;Korolev, S.N. Application of Satellite Data for Retrieving the Light Absorption Characteristics in the Black Sea Waters. *Physical Oceanography*2021, V. 28(2), pp. 205-214. https://doi.org/10.22449/1573-160X-2021-2-205-214

31. Korchemkina, E.N.; Shibanov, E.B.; Li, M.E. Improvement of the Atmospheric Correction Technique for Remote Investigations of Black Sea Coastal Waters. *Issled. Earth from space*2009, V. 6, pp. 24–30.

32. Wozniak, B., Dera, J., Light Absorption in Sea Water, *New York: Springer Science + Business Media*, 2007, 463 p.

33. Karabashev, G.S., Evdoshenko, M.A., On spectral indications of cyanobacterial blooms at ecologically different marine aquatic areas from satellite data, *Proceedings of 8th International Conference "Current Problems in the Optics of Natural Waters", St. Petersburg*, 2015, pp. 171–176.

34. Karabashev, G.S., Evdoshenko, M.A., Narrowband shortwave minima in spectra of backscattered light from the sea obtained from ocean color scanners as a remote indication of algal blooms, *Oceanologia*, 2016, Vol. 58, No. 5, pp. 279–291. URL: http://dx.doi.Org/10.1016/j.oceano.2016.05.001.

35. Karabashev, G. S., Evdoshenko, M. A. Short-wave minimum of water surface brightness coefficients as a satellite indicator of Nodularia spumigena "blooms" in the south of the Caspian Sea, *Modern problems of remote sensing of the Earth from space*, 2017, Vol. 14(1), p. 159).

36. Shybanov, E.B., Papkova, A.S. Algorithm for Additional Correction of Remote Sensing Reflectance in the Presence of Absorbing Aerosol. *Preprints.org*; 2022. DOI: 10.20944/preprints202211.0049.v1.